Journal of
Materials Chemistry B

Accepted Manuscript

This article can be cited before page numbers have been issued, to do this please use: L. Xu, X. He, Y. Huang, P. Ma, Y. Jiang, X. Liu, S. Tao, Y. Sun, D. Song and X. Wang, *J. Mater. Chem. B*, 2019, DOI: 10.1039/C8TB03230K.

ROYAL SOCIETY OF CHEMISTRY

rsc.li/materials-b

View Article Online
DOI: 10.1039/C8TB03230K

Journal Name

ARTICLE

A Novel Near-infrared Fluorescent Probe for Detecting Intracellular Alkaline Phosphatase and Imaging of Living Cells

Longbin Xu,[a] Xu He,[b] Yibing Huang,[b] Pinyi Ma,*[a] Yanxiao Jiang,[a] Xin Liu,[a] Shuo Tao,[c] Ying Sun,[a] Daqian Song,[a] and Xinghua Wang,*[a]

Received 00th January 20xx,
Accepted 00th January 20xx

DOI: 10.1039/x0xx00000x

www.rsc.org/

Development of novel near-infrared (NIR) fluorescent probes for the monitoring of active substances in living organism is desirable in biological studies. Herein, we designed a novel NIR MTR fluorophore which has longer emission wavelength, greater Stokes shift and higher quantum yield than the classic hemicyanine NIR fluorophore. The synthesized MTR-derived NIR probe (MTR-P) is highly selective and sensitive to alkaline phosphatase (ALP) activity. In the presence of ALP, MTR-P exhibited increased fluorescence signal by up to 56 folds at 723 nm, and it was determined to be 0.042 U L-1. In addition, the mechanism of MTR-P probe was further examined by HPLC, mass spectrometry and DFT/TDDFT calculation. The NIR probe MTR-P was successfully applied to measure the levels of alkaline phosphatase in different types of cells by fluorescence imaging.

Introduction

Small-molecule fluorescent probes can interact with analytes, such as cations, anions and human enzymes; accompanied by the changes of fluorescent spectral properties, they have become a powerful tool that can be used to detect or examine the analytes.[1, 2] Among these probes, near-infrared (NIR) fluorescent probe is high-demand ideal candidate for biological tissue imaging, owing to its various attractive advantages, which can include minimal damage to biological samples (the spectral are obtained in NIR region) and minimal interference from endogenous autofluorescence in living tissues.[3-7] Therefore, the probe not only has been extensively investigated, but also has been widely employed in many studies, such as in the study of spatial sampling capability by *in vivo* imaging.[8-10] Recently, numerous research have been devoted to engineer NIR fluorophores[11-14] (Figure 1), which have a number of limitations, including short stokes shifts, low fluorescence quantum yields, poor water solubility and bad photostability.[8] Accordingly, the fluorophores currently used for near-infrared light need to be further studied. Moreover, it can be beneficial to study fluorophores that show absorption and fluorescence emission spectra in the NIR region, and that can be detected *in vivo*.

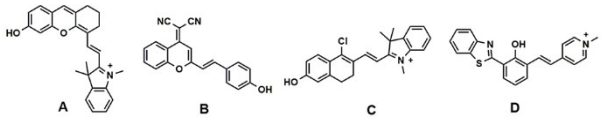

Figure 1 Common NIR fluorophore structures.

Alkaline phosphatase (ALP), which can be found in mammalian organs such as intestine, liver, bone, kidney, and placenta, is an enzyme catalyzing the hydrolysis.[15, 16] This enzyme is widely used as a biomarker for enzyme immunoassays and molecular biology.[17, 18] Abnormal ALP levels in organisms has been found to associate with the development and progression of various diseases such as prostate and breast cancers, and bone disease.[19-21] However, it remains unknown how ALP is involved in such pathological functions; thus, tracking ALP at the cellular level is crucial for obtaining such information. Accordingly, it is necessary to develop reliable, facile, and sensitive ALP analysis method to understand the mechanism of action of alkaline phosphatase in biological systems and to provide a basis for clinical diagnosis of related diseases.

A variety of spectroscopic methods for detecting ALP levels have been published, and these methods can include colorimetric,[22] fluorometric,[23] chromatographic,[24] and electrochemical[25] methods, as well as surface-enhanced resonance Raman scattering.[26] Nonetheless, these methods, except the fluorescence technique, usually require sample pretreatment and complex instrumentations, in addition to other limitations, such as low sensitivity of spectrophotometric methods and low repeatability of electrochemical methods.[15, 27, 28] The use of activatable fluorescence probes has a number of advantages, including high sensitivity, cost effectiveness, simplicity, and convenientness.[19,29-31] Therefore, small-molecule near-infrared (NIR) fluorescent probe can be advantageously used as analytical means for the detection of alkaline phosphatase in vivo.

[a] College of Chemistry, Jilin University, Qianjin Street 2699, Changchun 130012, China.
[b] College of Life Sciences, Jilin University, Qianjin Street 2699, Changchun 130012, China.
[c] Shandong Provincial Key Laboratory of Chemical Energy Storage and Novel Cell Technology, School of Chemistry and Chemical Engineering, Liaocheng University, Liaocheng 252059, China.
† Tel: +86 431 85168399; Fax: +86 431 85168399.
*E-mails: mapinyi@jlu.edu.cn (Pinyi Ma); starred.wang@gmail.com (Xinghua Wang).
Electronic Supplementary Information (ESI) available: [details of any supplementary information available should be included here]. See DOI: 10.1039/x0xx00000x

Herein, we designed a novel NIR fluorophore MTR which has longer emission wavelength, greater Stokes shift and higher quantum yield than the classic hemicyanine NIR fluorophore. The NIR fluorophore was synthesized by replacing 2,3,3-trimethyl-3H-indole in the classical hemicyanine dye with 2-methylbenzo[d]thiazole. For the first time, we developed a novel water-soluble ALP-sensitive fluorescent probe MTR-P which is used MTR as the platforms and modified a phosphate on the hydroxyl group. The MTR-P probe is nonfluorescent due to its phosphate group, which has both annihilation and recognition capabilities. Upon the addition of ALP, the emission of MTR-P at 723 nm was enhanced. Additionally, the probe exhibits good ALP-sensing performance with a linear range of 0-8 U L^{-1} (R^2 = 0.9971) and the detection limit of as low as 0.042 U L^{-1}; it also has excellent selectivity towards ALP. Moreover, MTR-P was successfully used for detecting the exogenous and endogenous alkaline phosphatase level in living cells.

Results and discussion

Design and synthesis of fluorophore MTR

Recently, the use of classic hemicyanine fluorophore to construct NIR fluorescent probes for in living cell imaging have attracted great attention.[32] However, these probes have disadvantages such as short Stokes shift, low fluorescence quantum yield and interference from scattered light. Hence, we synthesized a novel NIR fluorophore by replacing 2,3,3-trimethyl-3H-indole in the classical hemicyanine dye with 2-methylbenzo[d]thiazole.

The synthesized NIR fluorophore MTR (3-ethyl-2-(2-(6-hydroxy-2,3-dihydro-1H-xanthen-4-yl)vinyl)benzo[d]thiazol-3-ium) was then compared with the classic hemicyanine NIR fluorophore CyR (1-ethyl-2-(2-(6-hydroxy-2,3-dihydro-1H-xanthen-4-yl)vinyl)-3,3-dimethyl-3H-indol-1-ium). The photophysical properties were investigated H_2O/CH_3OH (99:1, v/v, 25 mM Tris-HCl buffer, pH=8.0), and the fluorescence spectra were recorded at an excitation (Ex=680 nm) and emission (Em) wavelengths between 690 nm and 850 nm (Ex/Em slit = 5/5 nm). As shown in Figure 2, the emission wavelength of CyR was 712 nm, whereas that of MTR was 723 nm. With the same excitation wavelength, a red shift to some degree of the emission peak was observed. Additionally, MTR (~43 nm) also have larger Stokes shift than CyR (~32 nm). Moreover, absolute quantum yield in CH_3OH of MTR (0.15) is higher than that of CyR (0.13), as demonstrated in Table 1. However, both MTR and CyR have the same relative light stability (Figure S1). Therefore, this indicates that the novel fluorophore MTR can have greater application potential than the hemicyanine NIR fluorophore CyR.

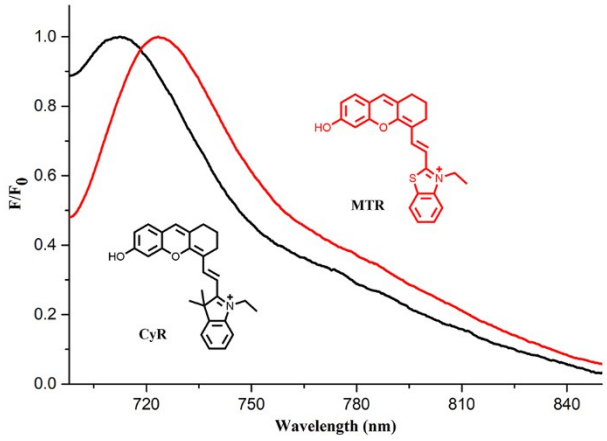

Figure 2 Fluorescence spectra of MTR (10 μM) and CyR (10 μM) in H_2O/CH_3OH (99:1, v/v, 25 mM Tris-HCl buffer, pH = 8.0).

Table 1 Common NIR fluorophore structures.

Dye	λ_{Ex}	λ_{Em}	Stokes shift	Φ
MTR	680 nm	723 nm	~43 nm	0.15
CyR	680 nm	712 nm	~32 nm	0.13

To better understand the luminescence behavior of probe CyR and MTR, we carried out computational studies. As shown in Figure 3, the HOMO and LUMO for both CyR and MTR probes are mainly distributed on the π-conjugated molecular framework, suggesting that the probe itself exhibits fluorescence properties. The LUMO → HOMO transition ($S_1 \rightarrow S_0$) in both probes are allowed with oscillator strength (f) of 1.1945 and 1.3904, and emission wavelengths of 710.05 nm and 722.67 nm, respectively, for CyR and MTR. This observation can be attributed to S atom in thiophene group, which has stronger electron-donating ability. The predicted emission spectra, obtained by TDDFT calculations, are also in good agreement with the predicted spectra. This further confirms that the MTR has better fluorescence character (longer emission wavelength and higher quantum yield) than its structural analogue CyR.

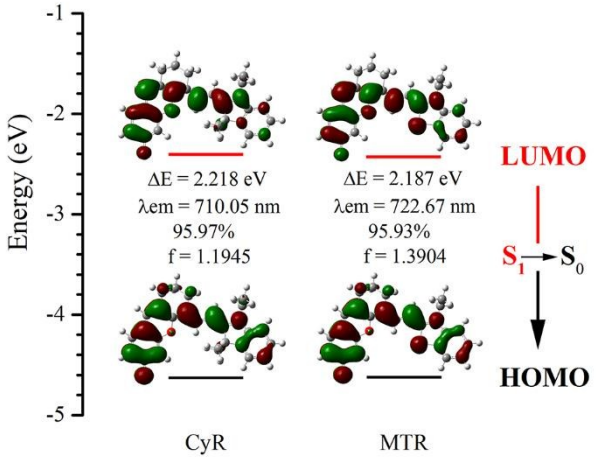

Figure 3 Optimized structures, HOMO−LUMO energy levels, wavelength, light harvesting efficiency (%), oscillator strength (f), and molecular orbital obtained from the emission spectra of CyR and MTR calculated by TDDFT using the optimal structures at the first excited states.

Spectroscopic Properties of MTR-P to ALP

Because pH is a significant factor affecting enzyme reaction, the pH-dependent response of the probe was determined in Tris-HCl buffer (Figure S2). The MTR-P probe (10 μM) exhibits good response to ALP (10 U L^{-1}) at the pH range of 2.0 to 10.0. Considering both the enzyme activity and the bioimaging, the optimum pH of 8.0 was selected for subsequent experiments. Time, which is another factor affecting the MTR-P probe, was also examined. After the probe was treated with ALP (10 U L^{-1}), its fluorescence emission wavelength at 723 nm was measured within 0 to 20 min, and we observed that stable readings of intensity could be acquired within 15 min (Figure S3). Once a stable value was reached, the fluorescence intensity became

relatively stable. Therefore, the determination of fluorescence intensity was carried out within 15 min after ALP was added.

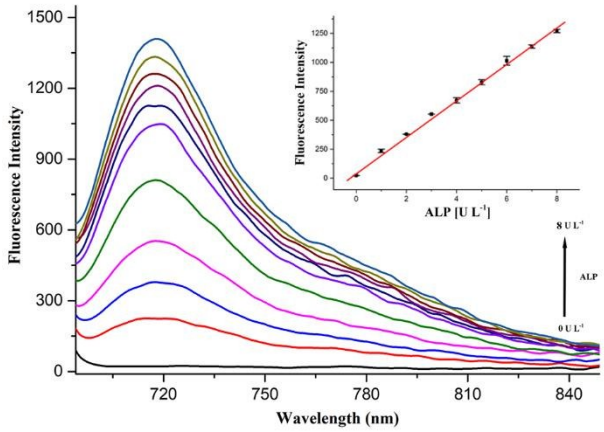

Figure 4 Fluorescence spectra of MTR-P (10 μM) in 25 mM Tris-HCl buffer, pH = 8.0, upon the addition of ALP (0, 1, 2, 3, 4, 5, 6, 7, and 8 U L^{-1}). Inset: a plot of fluorescence intensity versus ALP concentration.

Furthermore, the concentration-dependent response of the probe upon stepwise addition of ALP was examined. The intensity of fluorescence emission increases progressively by about 56-folds after the concentration of ALP was increased up to 10 U L^{-1} (the concentration of MTR-P was kept constant at 10 μM; Figure 4). The inset of Figure 4 (Figure S4) shows that the fluorescence emission is linearly proportional to the ALP concentration from 0 to 8 U L^{-1}, and the detection limit was 0.042 U L^{-1} (3σ/k). In addition, the regression equation was determined as y=153.96x+63.262 with R=0.9971 and σ=2.16. The experimental data further proves that the NIR MTR-P probe can potentially detect ALP under the simulated physiological conditions. The probe MTR-P exhibited preeminent sensitivity compared to the previously reported fluorescent probes (Table S1).

The NIR MTR-P probe not only can detect the ALP activity, but also can potentially be used for the screening of enzymes inhibitors. Thus, the effect of various concentrations of Na_3VO_4, a well-known inhibitor of ALP, on the probe was investigated. The MTR-P probe (10 μM) was added to ALP solution (10 U L^{-1}) previously incubated with different concentrations of Na_3VO_4 (0-300 μM) for 10 min. The emission at 723 nm gradually decreases with increasing concentration of Na_3VO_4 (Figure S5). The calculated IC_{50} for Na_3VO_4 is 23.98 μM, which is in good agreement with the previously reported value.[33] Therefore, MTR-P can potentially be used to screen ALP inhibitors.

Selectivity of MTR-P Probe

The selectivity of MTR-P probe to ALP was researched to evaluate the use of MTR-P for selective binding to ALP. Fluorescent responses of the probe to a wide range of enzymes and anions (including ALP, ACP, Met, His, Arg, PHE, Ser, Hcy, GGT, UA, Fe^{2+}, Co^{2+}, AchE, Tyr, GOD, GSH, Cys, BSA, AA, IgG, F^-, Cl^-, Br^-, I^-, SO_3^{2-}, and CN^-) were measured. The analytes were incubated with MTR-P for 15 min and their fluorescent intensity changes (due to MTR-P) were measured. Figure 5 shows the fluorescent spectra and the corresponding bar plot. The fluorescent signal is remarkably enhanced when ALP (10 U L^{-1}) is present, and it appears that interferences have no effect on the fluorescent signal of the probe. Among all analytes, ADP only causes a slight enhance of fluorescence; the change is at a much lesser extent. These results further signify that the MTR-P probe is highly selective to ALP, and thus has a promising potential for detecting ALP in living cells without any interferences. Then, the competition (interference) experiments were further conducted using the above analytes and ALP. The data showed that the interferences by these analytes have little or no effects on the detection of ALP, thus undoubtedly indicating that MTR-P is highly selective to ALP.

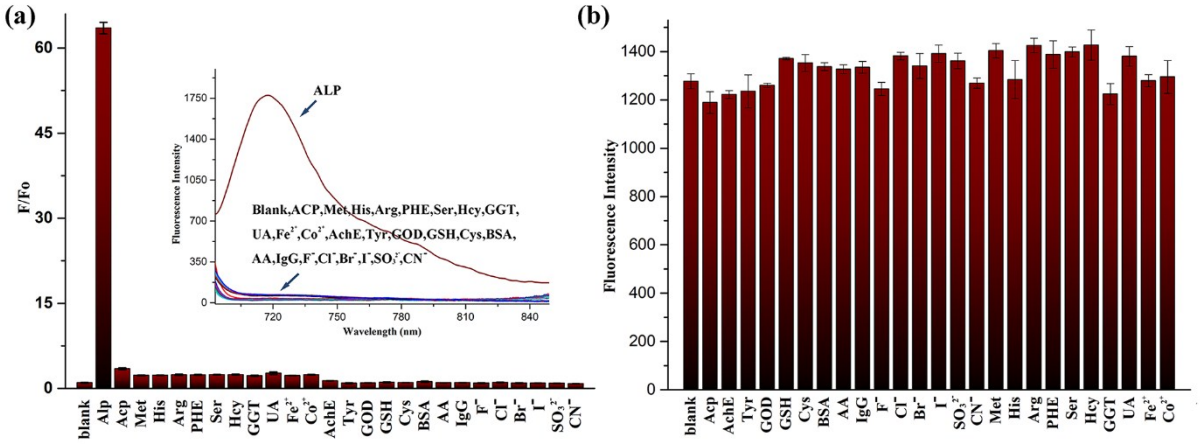

Figure 5 (a) Fluorescence response of MTR-P (10 μM) upon the addition of ALP (10 U L^{-1}), ACP (10 U L^{-1}), and other interferences including: 100 μM each of Met, His, Arg, PHE, Ser, Hcy, UA, Fe^{2+}, Co^{2+}, GSH, Cys, AA, F^-, Cl^-, Br^-, I^-, SO_3^{2-}, and CN^-; 100 U L^{-1} each of GGT, AchE, Tyr, and GOD; and 100 mg L^{-1} each of BSA and IgG. The probe was dissolved in Tris-HCl buffer (25 mM, pH = 8.0). Inset: Fluorescence spectra of MTR-P (10 μM) in the presence of ALP (10 U L^{-1}) and other interferences. (b) Fluorescence response of MTR-P (10 μM) upon the addition of interferences including: ACP (10 U L^{-1}); 100 μM each of Met, His, Arg, PHE, Ser, Hcy, UA, Fe^{2+}, Co^{2+}, GSH, Cys, AA, F^-, Cl^-, Br^-, I^-, $SO3^{2-}$, and CN^-; 100 U L^{-1} each of GGT, AchE, Tyr, and GOD; and 100 mg L^{-1} each of BSA and IgG, in Tris-HCl buffer (25 mM, pH = 8.0) and the presence of ALP (10 U L^{-1}).

View Article Online
DOI: 10.1039/C8TB03230K

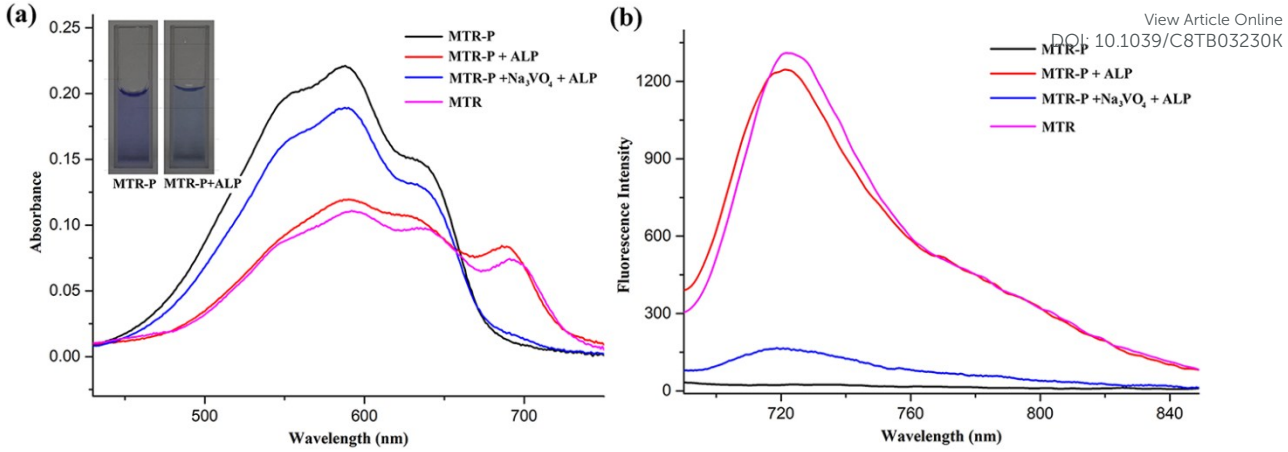

Figure 6 (a) Absorption and (b) fluorescence spectra of MTR (10 μM), MTR-P (10 μM) in the presence and absence of ALP (20 U L^{-1}), and MTR (10 μM) in the presence of ALP (20 U L^{-1}) and its inhibitor Na_3VO_4 (100 μM). The samples were in Tris-HCl buffer (25 mM, pH = 8.0).

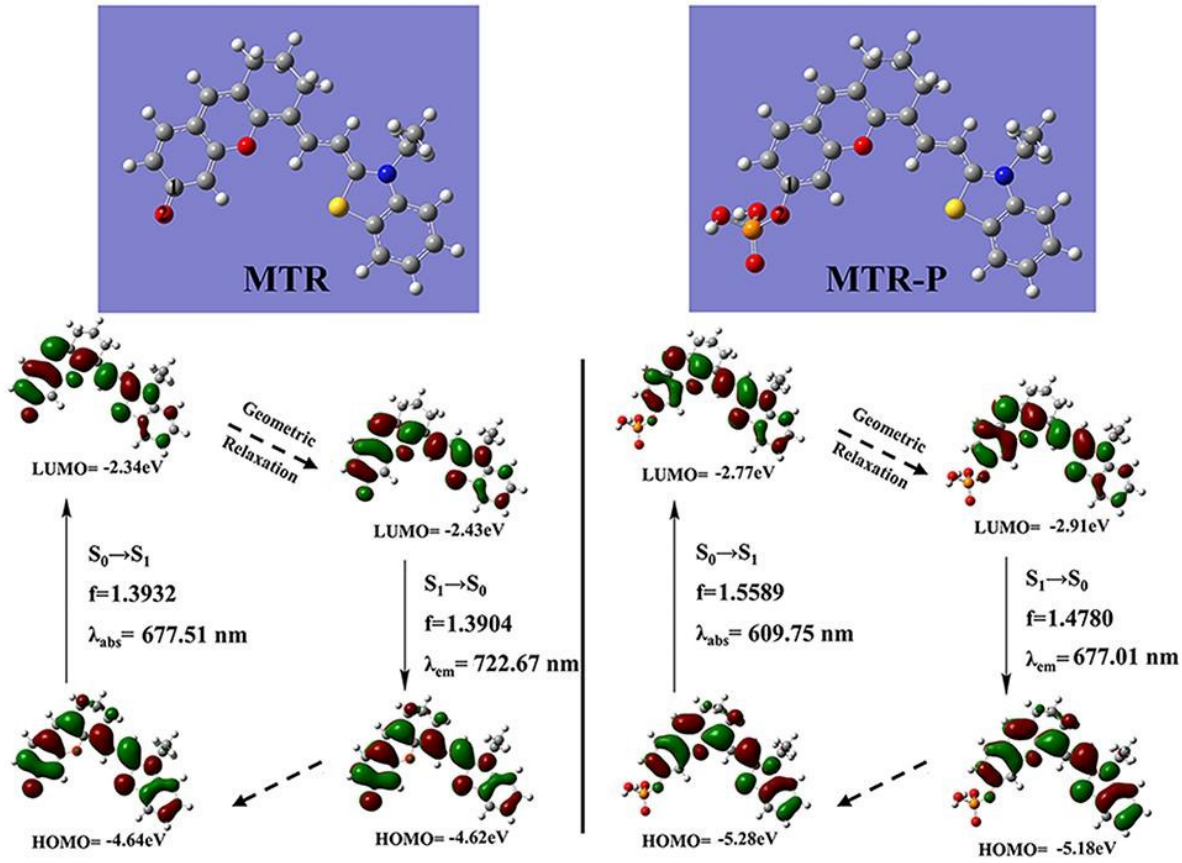

Figure 7 Theoretical molding of MTR and MTR-P calculated by TDDFT using the optimal structures of the ground and the first excited states. The structures are illustrated with their corresponding vertical excitation energy, oscillator strength (f), recognition process, wavelength, and relevant frontier molecular orbits.

Sensing Mechanism of MTR-P Toward ALP

The photophysical properties of MTR-P were investigated in Tris-HCl buffer solution (25 mM, pH = 8.0) with or without ALP (20 U L^{-1}). In Figure 6a, MTR-P (20 μM) in Tris-HCl buffer has a maximum absorption at 588 nm. In the presence of ALP (20 U L^{-1}), the absorption band MTR-P was significantly decreased to center at 588 nm, while the absorption band was increased to center at 658 nm. Similarly to MTR, the color of the mixture was changed from purplish to cyan after 15 min. The absorption spectrum of MTR-P (20 μM) containing ALP (20 U L^{-1}) and its inhibitor Na_3VO_4 (100 μM) is similar to that of MTR-P. Free MTR-P probe in aqueous solution exhibited very weak fluorescence over the emission wavelength range of 690 to 850 nm (Figure 6b). However, with the addition of ALP (20 U L^{-1}), the emission spectra were enhanced to center at 723 nm after 15 min; this observation is the same as that observed for MTR. These data demonstrate that the addition of ALP (20 U L^{-1}) and its inhibitor Na_3VO_4 (100 μM) into MTR-P (20 μM) causes only slight changes in

fluorescence spectra, indicating that ALP is able to effectively remove phosphate groups from MTR-P, converting it to MTR.

To further investigate the sensing mechanism of the probe, MTR-P with ALP (20 U L^{-1}) in Tris-HCl buffer was subjected to MS analysis. The peak at m/z = 468.4279 corresponding to MTR-P was decreased, while that at m/z = 388.4432 corresponding to MTR was appeared (Figure S6). In addition, the HPLC analysis showed a peak associated with MTR-P at 5.47 min, and a peak corresponding to MTR at 7.19 min (Figure S7). After ALP was added into MTR-P, the peak at 5.47 min was disappeared, and a new peak corresponding to MTR at 7.33 min was appeared. These results demonstrate that the ability to remove phosphate groups of alkaline phosphatase can transform the MTR-P into fluorophore MTR and simultaneously causing changes in ultraviolet and fluorescent signals (Scheme 1).

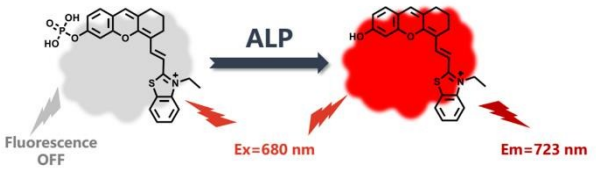

Scheme 1 Proposed reaction mechanism of the fluorometric assay for ALP activity with MTR-P.

To gain insights into the enhanced fluorescence of MTR-P in the presence of alkaline phosphatase, the electronic and optical properties, and structures of MTR-P and MTR were calculated using DFT and TDDFT methods (Figure 7). MTR has a C(1)–O(2) bond length of 127.1 pm, which is similar to the bond length of C=O double bond (~121 pm); this indicates that there is electron drawing from O(2) atom to π-conjugated system. ICT can be achieved from benzothiazole (donor) in MTR to xanthine (receptor); as a result, a push-pull electronic conjugate system was constructed. The TDDFT calculation results further show that the main absorption peak of MTR is at 677.51 with f = 1.3932 (oscillator strengths), and the main fluorescence emission peak is at 722.67 with f = 1.3904. This indicates that MTR can emit strong fluorescence signal. On the other hand, the bond length between C(1)–O(2) in MTR-P is 139.7 p.m, which matches the bond length of C–O single bond (~144 p.m.). This may be due to the weakening of p–π conjugation between O(2) atom and π-conjugated xanthylium framework. Compared to MTR, although contribution to the HOMO/LUMO of O(2) atom in MTR-P is less than that in MTR, its HOMO and LUMO energy levels is higher. The results from theoretical calculations indicated that the O(2) atom in MTR-P had lower electron donating ability due to phosphate, and it can be hinder the ICT mechanism in the MTR. The TDDFT calculation of MTR-P showed that the main absorption and fluorescence emission peaks are 609.75 nm (f = 1.5589) and 677.01 nm (f = 1.4780), respectively. Because the emission peak is blue shifted to overlap with the Rayleigh scattering peak, the fluorescence peak for MTR-P was not observed. Altogether, the theoretical calculations are consistent with the experimental data.

These experimental results confirm that the destruction of phosphorus and oxygen bonds in MTR-P can lead to significant increased fluorescent signals in the near-infrared region.

Fluorescence Imaging of ALP in Living Cells

Prior to fluorescence imaging, the cytotoxicity of MTR-P to BEL 7402 cells was examined by MTT assays. As shown in Figure S8, after the cells were cultured with 20 μM MTR-P for 24 h, cell viability remained high, indicating that the probe exhibits low cytotoxicity to the cells. Encouraged by its low cytotoxicity, MTR-P was further used for detecting the levels of exogenous and endogenous alkaline phosphatase in HEK 293T and BEL 7402 cells.

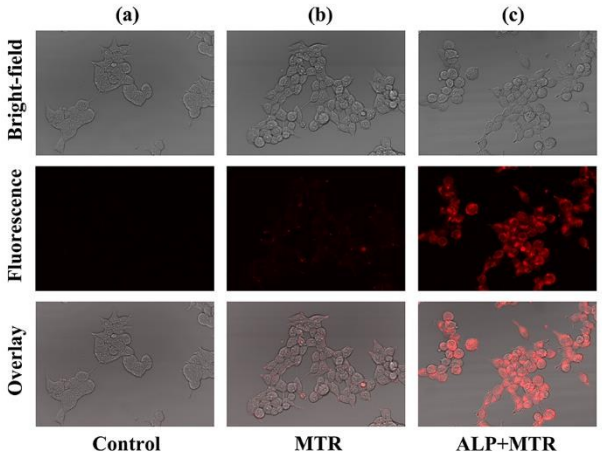

Figure 8 Fluorescence images of HEK 293T cells. From left to right: control; cells treated with MTR-P (10 μM); and cells treated with ALP (10 U L^{-1}), followed by MTR-P (10 μM).

HEK 293T cells were used as an exogenous model because they express low amount of ALP. As shown in Figure 8a, with the excitation at 635 nm, HEK 293T did not exhibit background fluorescence signal. Following the cells were incubated with 10 μM MTR-P for 15 min and washed thoroughly (to remove excess MTR-P) prior to cell imaging, the fluorescence signal inside HEK 293T cells remains low (Figure 8b). By contrast, significant red fluorescence signal was observed from the cells treated with ALP (10 U L^{-1}) for 15 min, followed by MTR-P (10 μM) for 15 min (Figure 8c). The fluorescence intensities from the corresponding HEK 293T cells were shown in Figure S9. This observation indicates that the MTR-P probe can be used to monitor the levels of enzymatic activity of exogenous ALP in living cells.

Encouraged by these results, we further used MTR-P to detect the levels of endogenous ALP in living cells. Human hepatoma BEL 7402 cell line was chosen as a representative cell line because it has overexpression of ALP which could cause higher risk of liver disease [34]. With the excitation at 635 nm, untreated BEL 7402 cells did not exhibit background fluorescence signal (Figure 9a), whereas the cells treated with MTR-P (10 μM) for 15 min exhibited strong fluorescence signal (Figure 9b). To further verify whether or not the fluorescence signal can be affected by ALP, and its inhibitor Na_3VO_4 (50 μM), the cells were treated with ALP and Na_3VO_4 for 15 min prior to incubating with MTR-P (10 μM) for additional 15 min; and the results showed that the fluorescence signal was not distinctly observed (Figure 9c). On the other hand, BEL 7402 cells treated with Na_3VO_4 (50 μM) for 15 min, followed by ALP (10 U L^{-1}) for 15 min, MTR-P (10 μM) for 15 min exhibited strong fluorescence signal (Figure 9d). And the fluorescence intensities from the corresponding HEK 293T cells were shown in Figure S10. These observations suggest that the MTR-P can efficiently and effectively detect the endogenous alkaline phosphatase levels in living cells.

Taken together, these results indicate that the probe MTR-P can effectively and efficiently detect exogenous and endogenous ALP activity in living cells.

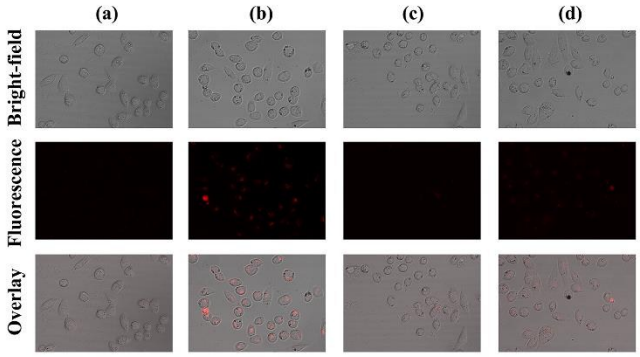

Figure 9 Fluorescence images of BEL 7402 cells. From left to right: control; cells treated with MTR-P (10 μM); cells treated with Na_3VO_4 (50 μM), followed by MTR-P (10 μM); and cells treated with Na_3VO_4 (50 μM), followed by ALP (10 U L^{-1}) and MTR-P (10 μM).

Experimental

Synthesis

Scheme 2 depicts the synthetic route to compounds, which can be found in the supplementary material. (^{1}H NMR, ^{13}C NMR, and MS spectra can be found in Figures S11-S28).

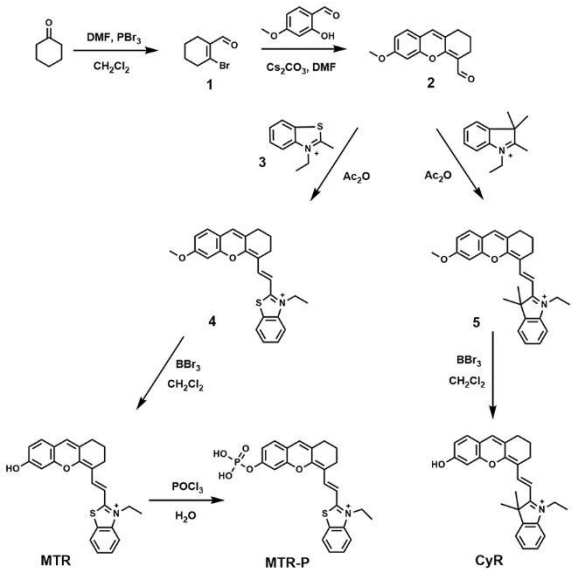

Scheme 2. Synthetic route of the probe.

Synthesis of **MTR-P**

To a reactant of MTR (0.1 g, 0.25 mmol) in anhydrous pyridine (3 mL) was cooled down to 0 °C. After that, phosphorus oxychloride (0.1 mL) was slowly added to the reactants under vigorous stirring. The solution was stirred at room temperature for 6 h; after that, it was poured into ice and then stirred for another 12 h. Subsequently, the solution was evaporated to remove the solvent, and then purified by silica gel column chromatography (CH_2Cl_2:CH_3OH=5:1 v/v); and a dark purple solid was obtained. Yield: 0.052 g (43.2 %). ^{1}H (500 MHz, CD_3OD): δ 8.53 (1H, d), 8.03 (1H, m), 7.78 (2H, d), 7.41 (1H, s), 7.33 (1H, d), 7.10 (2H, d), 6.82 (1H, d), 5.43 – 5.29 (2H, m), 2.72 (4 H, d), 0.92 (5 H, t). ^{31}P NMR (243 MHz, DMSO-d6) δ = -5.34. MS (ESI, m/z) calcd for $[C_{24}H_{23}NO_5PS]^+$: 468.10, found: 468.44.

Fluorescence Measurements

The measurement of FL and UV-vis spectra were carried out as follows. A stock solution of MTR-P (20 μM) was prepared in Tris-HCl buffer (25 mM, pH = 8.0, 1 mM $MgCl_2$). Preparation of various concentrations of ALP was carried out by dissolving ALP in Tris-HCl buffer (25 mM, pH = 8.0, 1 mM $MgCl_2$). Different concentrations of amino acid, cations and other interfering substance were also prepared using the method used for preparing ALP stock solution. Then, the test solution was obtained by mixing 0.5 mL stock solution of MTR-P and 0.5 mL stock solution of ALP or interfering substances. After that, the resultant solution was shaken at 25 °C for 15 min, and its spectral properties were then measured. The fluorescence spectra were measured with the excitation at 680 nm and emission wavelength ranges of 690 to 850 nm.

Theoretical Calculation and Analysis

The optimal geometrical and electronic structures of the probes were determined by the DFT (density functional theory) and B3LYP/6-31G(d) basis sets using Gaussian 16 software.[35] The UV-vis and FL spectra for each calculation were recorded at the time-dependent DFT (TDDFT) by optimizing S_0 (the energy level of ground state) and S_1 (the energy level of the first excited state) structures. The effect of solvent was calculated by SMD model, and water was used as the solvent in the calculation.

Cell Incubation and Imaging

HEK 293T and BEL 7402 cells, which was also obtained from the Life Sciences College of Jilin University (Jilin, China), were grown in DMEM (Dulbecco's modified Eagle medium) supplemented with 10 % heat-inactivated fetal bovine serum (FBS) at 37 °C under 5% CO_2 atmosphere. After washing several times with PBS buffer (pH = 7.2-7.4), the cells were incubated with 10 μM MTR-P probe dissolved in PBS for 15 min. As control groups, BEL 7402 cells were pretreated with Na_3VO_4 (50 μM), whereas HEK 293T cells were pretreated with ALP (10 U L^{-1}). After the pretreatment for 20 min, the cells were incubated with MTR-P (10 μM) for additional 15 min. As an additional control group, BEL 7402 cells were also treated with Na_3VO_4 (50 μM) for 20 min, followed by ALP (10 U L^{-1}) for additional 15 min. After that, the cells were incubated with the MTR-P (10 μM) for additional 15 min. The cells were observed under a confocal fluorescence microscope at an excitation wavelength of 635 nm and imaged by a confocal fluorescence microscope with the emission wavelengths between 680 and 750 nm.

Conclusions

We successfully synthesized hemicyanine dye-mimic NIR MTR by replacing 2,3,3-trimethyl-3H-indole with 2-methylbenzo[d]thiazole. The synthesized NIR MTR fluorophore has longer emission wavelength, larger stokes shifts and stronger fluorescence quantum yields compared with hemicyanine fluorophore CyR. The MTR was further designed (denoted as MTR-P) and applied to detect the activity of ALP. The MTR-P probe exhibits good ALP-sensing performance with the linear range of 0-8 U L^{-1} (R^2 = 0.9971) and the detection limit is 0.042 U L^{-1}, which is lower than most of other ALP probes previously reported. The luminescence and detection

mechanisms of MTR-P probe upon the addition of ALP were also investigated by UV-vis and fluorescent spectroscopy, mass spectrometry, theoretical calculation, and HPLC. Furthermore, the MTR-P was successfully applied to probe the exogenous and endogenous alkaline phosphatase activity in living cells. These findings demonstrate the established probe has a promising application potential in simplifying clinical diagnosis of both liver and bone diseases.

Conflicts of interest

There are no conflicts to declare.

Acknowledgements

This work was supported by the National Natural Science Foundation of China (Nos. 21405057 and 21207047), Science and Technology Developing Foundation of Jilin Province of China (Nos. 20180201050YY and 201701011106JC), Industrial Innovation Funds of Jilin Province of China (No. 2018C034-1), Project of the Education Department of Jilin Province of China (No. 2016411).

Notes and references

1. X. Li, X. Gao, W. Shi and H. Ma, *Chemical Reviews*, 2014, **114**, 590-659.
2. X. Chen, M. Sun and H. Ma, *Current Organic Chemistry*, 2006, **10**, 477-489.
3. C.-H. Quek and K. W. Leong, *Nanomaterials*, 2012, **2**, 92.
4. C. S. Park, T. H. Ha, M. Kim, N. Raja, H.-s. Yun, M. J. Sung, O. S. Kwon, H. Yoon and C.-S. Lee, *Biosensors and Bioelectronics*, 2018, **105**, 151-158.
5. F. Yu, P. Li, G. Li, G. Zhao, T. Chu and K. Han, *Journal of the American Chemical Society*, 2011, **133**, 11030-11033.
6. F. Yu, P. Li, B. Wang and K. Han, *Journal of the American Chemical Society*, 2013, **135**, 7674-7680.
7. Z. Lou, P. Li and K. Han, *Accounts of Chemical Research*, 2015, **48**, 1358-1368.
8. H. Chen, B. Dong, Y. Tang and W. Lin, *Accounts of Chemical Research*, 2017, **50**, 1410-1422.
9. X. Han, F. Yu, X. Song and L. Chen, *Chemical Science*, 2016, **7**, 5098-5107.
10. Y. Huang, F. Yu, J. Wang and L. Chen, *Analytical Chemistry*, 2016, **88**, 4122-4129.
11. J. Deng, P. Yu, Y. Wang and L. Mao, *Analytical Chemistry*, 2015, **87**, 3080-3086.
12. J. Wang, B. Li, W. Zhao, X. Zhang, X. Luo, M. E. Corkins, S. L. Cole, C. Wang, Y. Xiao, X. Bi, Y. Pang, C. A. McElroy, A. J. Bird and Y. Dong, *ACS Sensors*, 2016, **1**, 882-887.
13. H. Chen, Y. Tang, M. Ren and W. Lin, *Chemical Science*, 2016, **7**, 1896-1903.
14. P. Xu, T. Gao, M. Liu, H. Zhang and W. Zeng, *Analyst*, 2015, **140**, 1814-1816.
15. L. Zhao, S. Xie, X. Song, J. Wei, Z. Zhang and X. Li, *Biosensors and Bioelectronics*, 2017, **91**, 217-224.
16. X. Hou, Q. Yu, F. Zeng, J. Ye and S. Wu, *Journal of Materials Chemistry B*, 2015, **3**, 1042-1048.
17. F. Zheng, S. Guo, F. Zeng, J. Li and S. Wu, *Analytical Chemistry*, 2014, **86**, 9873-9879.
18. J. E. Coleman, *Annu. Rev. Biophys. Biomol. Struct*, 1992, 441-483.
19. T. Xiao, J. Sun, J. Zhao, S. Wang, G. Liu and X. Yang, *ACS Applied Materials & Interfaces*, 2018, **10**, 6560-6569.
20. J. A. Lorente, H. Valenzuela, J. Morote and A. Gelabert, *European Journal of Nuclear Medicine*, 1999, **26**, 625-632.
21. Fernandez, Nicole J. and B. A. Kidney, *Veterinary Clinical Pathology*, 2007, **36**, 223-233.
22. Y. Choi, N.-H. Ho and C.-H. Tung, *Angewandte Chemie*, 2007, **119**, 721-723.
23. Y. Tan, L. Zhang, K. H. Man, R. Peltier, G. Chen, H. Zhang, L. Zhou, F. Wang, D. Ho, S. Q. Yao, Y. Hu and H. Sun, *ACS Applied Materials & Interfaces*, 2017, **9**, 6796-6803.
24. H. Takuya, S. Masaru, T. Kohei, M. Hirotaka, U. Tomonari and H. Hiroki, *Bulletin of the Chemical Society of Japan*, 2006, **79**, 1211-1214.
25. T. Murata, T. Yasukawa, H. Shiku and T. Matsue, *Biosensors and Bioelectronics*, 2009, **25**, 913-919.
26. C. Ruan, W. Wang and B. Gu, *Analytical Chemistry*, 2006, **78**, 3379-3384.
27. H. Zhang, C. Xu, J. Liu, X. Li, L. Guo and X. Li, *Chemical Communications*, 2015, **51**, 7031-7034.
28. H. Zhang, R. Liu, J. Liu, L. Li, P. Wang, S. Q. Yao, Z. Xu and H. Sun, *Chemical Science*, 2016, **7**, 256-260.
29. Y. Liu and K. S. Schanze, *Analytical Chemistry*, 2008, **80**, 8605-8612.
30. T.-I. Kim, H. Kim, Y. Choi and Y. Kim, *Chemical Communications*, 2011, **47**, 9825-9827.
31. S.-J. Li, C.-Y. Li, Y.-F. Li, J. Fei, P. Wu, B. Yang, J. Ou-Yang and S.-X. Nie, *Analytical Chemistry*, 2017, **89**, 6854-6860.
32. S.-Y. Liu, H. Xiong, J.-Q. Yang, S.-H. Yang, Y. Li, W.-C. Yang and G.-F. Yang, *ACS Sensors*, 2018, **3**, 2118-2128.
33. J. Zhao, S. Wang, S. Lu, X. Bao, J. Sun and X. Yang, *Analytical Chemistry*, 2018, **90**, 7754-7760.
34. F. Zhang, X. He, P. Ma, Y. Sun, X. Wang and D. Song, *Talanta*, 2018, **189**, 411-417.
35. M. J. Frisch, G. W. Trucks, H. B. Schlegel, G. E. Scuseria, M. A. Robb and J. R. Cheeseman, *Gaussian 16, Revision A. 03, Gaussian Inc., Wallingford CT*, 2016.

View Article Online
DOI: 10.1039/C8TB03230K

Table of contents entry

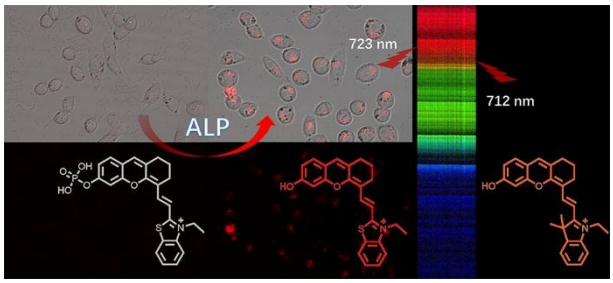

Design, Synthesis and application of fluorescent probe with novel near-Infrared fluorophore for in vivo imaging of alkaline phosphatase.